Small Ice Crystals in Cirrus Clouds: A Model Study and Comparison with In Situ Observations

HONG LIN

Atmospheric Environment Service, Downsview, Ontario, Canada

KEVIN J. NOONE AND JOHAN STRÖM

Department of Meteorology, Stockholm University, Stockholm, Sweden

ANDREW J. HEYMSFIELD

National Center for Atmospheric Research, Boulder, Colorado

(Manuscript received 22 March 1996, in final form 5 September 1997)

ABSTRACT

An air parcel model including homogeneous freezing nucleation of ice crystals has been used to study the formation and development of cirrus clouds. In situ measurements taken during March 1994 over southern Germany were used for comparison with model predictions. Typical experimental data were chosen for a base-case model run. Using measured aerosol properties as input values, the model predicts the measured ice crystal size distribution. In particular, both measurements and model results show the presence of numerous small ice crystals (diameter between 1 and 20 μm). Both measurements and model results also show that small aerosol particles (below 0.1 μm diameter) are active in forming cirrus cloud particles. The modeled microphysical properties including ice crystal size distribution, number concentration, and the residual particle size distribution are in good agreement with the experimental data. Based on the measured parameter values, a model sensitivity study considering air parcel updraft velocity, initial temperature, relative humidity, aerosol size distribution, number concentration, and air parcel vertical displacement is presented.

1. Introduction

Cirrus clouds cover about 20%–50% of the earth's surface and have a major effect on climate through their influence on the earth's radiative balance. The radiative properties of cirrus clouds depend on their ice water content, ice crystal size distribution, crystal shapes, number concentrations, and other microphysical properties (Liou 1986). Recently, the occurrence of small crystals in cirrus clouds and their radiative properties began to attract the attention of researchers. A modeling study by Zender and Kiehl (1994) showed that the shortwave forcing and albedo were very sensitive to the presence of small crystals (3–20 μm) in cirrus clouds. In a cirrus cloud radiative transfer study, Kinne et al. (1992) found that it is difficult to explain the discrepancies between modeled cirrus radiative fluxes with experimental measurements without including small crystals ($<$50 μm) in their model.

Corresponding author address: Dr. Hong Lin, Cloud Physics Research Division, Atmospheric Environment Service, 4905 Dufferin Street, Downsview, ON M3H 5T4, Canada.
E-mail: lin@armph3.tor.ec.gc.ca

The characteristics of cirrus ice crystal size distributions and associated size spectral moments have been reported in a number of studies. The results have been presented in summaries by Liou (1986) and Dowling and Radke (1990). However, measurements of size spectra for ice crystals around or smaller than 20 μm have previously been either unavailable or, in many cases, unreliable. The existence of high concentrations of small crystals ($\leq$30 μm) was seldom reported until recently by Noone et al. (1993), Ström et al. (1994a), Ström and Heizenberg (1994), and Ström et al. (1997).

Modeling studies have been performed to investigate cirrus cloud formation processes (e.g., Starr and Cox 1985; Heymsfield and Sabin 1989; Sassen and Dodd 1989; Jensen et al. 1994a,b; DeMott et al. 1994). The formation processes of ice crystals can be divided into homogeneous nucleation and heterogeneous nucleation. Homogeneous nucleation refers to the spontaneous freezing of a supercooled droplet at sufficiently low temperature, without the involvement of ice nuclei. Heterogeneous nucleation implies ice crystal formation initiated by ice nuclei, either by direct deposition of water vapor onto ice nuclei or enhancement of supercooled droplet freezing rates by ice nuclei (e.g., contact and

immersion freezing, condensation freezing) (Heymsfield and Sabin 1989; DeMott et al. 1994). A leading theory on the nature of ice crystal nucleation in cirrus clouds is that ice crystals form by homogeneous freezing of solution droplets. Homogeneous nucleation appears to be the dominant ice formation mechanism in the upper troposphere (Jensen et al. 1994a).

In this paper, an existing cirrus cloud microphysical model developed by Heymsfield and Sabin (1989) has been adapted to accept measured aerosol size distributions as inputs to study the formation of small crystals in cirrus clouds. Representative data selected from a measurement campaign carried out over southern Germany during March 1994 (Ström et al. 1997) were used for a base-case model run. Additionally, sensitivity tests were performed using a selected range of measured parameter values. The modeled microphysical properties that were compared with measurements included ice crystal size distribution, number concentration, condensed water content, and the properties of the scavenged aerosol particles. The study also includes a discussion of the parameters in the model for which the predicted cloud microphysics appears to be most sensitive.

2. Cirrus model

The cirrus model used in this study was originally developed by Heymsfield and Sabin (1989). This model has been used previously in an orographic wave cloud study, where the temperature was low (<-30°C) and vertical updraft was strong (>2 m s^{-1}; Heymsfield and Miloshevich 1993), and also in a study of the influence of relative humidity and temperature on cirrus formation (Heymsfield and Miloshevich 1995). Their results were compared with in situ measurements and have shown the importance of homogeneous nucleation processes on crystal formation at lower temperatures.

The model consists of a system of ordinary differential equations [see Heymsfield and Sabin (1989) for detailed description] that describe both the microphysical properties of the droplets and ice crystals, and the macrophysical properties of the rising air parcel. The model is set up as an initial value problem. Starting values for each of the parameters, including pressure, temperature, relative humidity, and updraft velocity are chosen from measurements. The model has been adapted to accept aerosol size distributions as inputs instead of using assumed cloud condensation nuclei (CCN) spectra to generate input aerosol size distributions (Heymsfield and Sabin 1989). Measured aerosol size distributions were directly used as an input for the simulations. Aerosol particles between 0.005 and 3 μm diameter are divided into 25 size bins. The model simulation begins when aerosol particles deliquesce in the air parcel. The aerosol particles are assumed to be composed of ammonium sulfate and to be completely soluble. These particles are allowed to grow to equilibrium size before lifting. The updraft velocity of the air parcel is held constant throughout the calculation. As the parcel rises, the solution droplets continue to grow by water vapor diffusion. When the temperature becomes sufficiently low, ice crystals start to nucleate by homogeneous freezing of the solution droplets. At each simulation time step, droplet growth and evaporation, and crystal nucleation and growth are calculated. Aerosol particles within each droplet or crystal are also followed.

3. Measurement data

In situ measurements made in synoptic frontal cirrostratus over southern Germany in March 1994 (Ström et al. 1997) were used as a basis for model simulation. The observations were made by the German research aircraft *Falcon.* Four flights were conducted on 18, 22, and 25 (two flights) March 1994 in an area bounded by latitude 47°N and 50°N, and longitude 11°E and 15°E over southern Germany. Cirrus microphysical properties and meteorological data were recorded during the flights. The aircraft instrumentation included a CVI (Counterflow Virtual Impactor) payload (Ogren et al. 1985; Noone et al. 1988; Lin and Heintzenberg 1995) together with an interstitial inlet (Schröder and Ström 1995), an ice replicator (Hallett 1976), and meteorological sensors. The ice replicator provided images of ice crystals from which crystal number and size distributions were derived. The sampling characteristics of the replicator are not well known. However, simple calculation yields a 50% sampling efficiency of around 4 μm diameter. The CVI payload consists of a CVI inlet, an interstitial inlet, and instruments downstream. CVI inlet has a cut size of about 5 μm (Lin and Heintzenberg 1995; Lin and Noone 1996). It provides information on the concentration and mean size of cloud particles, the concentration and size distribution of residual aerosol particles (particles left behind after evaporation of the cloud particles), and cloud water content. Interstitial inlet measures interstitial aerosol particles smaller than about 1 μm diameter (Schröder and Ström 1995). A detailed description of the measurements that we will use for our model calculations and the techniques used to make them is presented in Ström et al. (1997). Only a brief description of some of the instruments will be given here when necessary.

a. Model input parameters

The model requires a complete specification of the initial conditions, including pressure, temperature, relative humidity, updraft velocity, and aerosol properties. In situ observations were used to initialize the model predictions. We chose the cirrus observed in a flight on 18 March 1994 as our base-case study. A range of initial input, based on the measurements from all four flights of the campaign, was also selected for sensitivity study. The values are given in Table 1.

TABLE 1. Model input values. The base case best represents measurements taken from one flight on 18 March 1994. The upper and lower limits are chosen based on measurements from all four flights of the experiment for model sensitivity study.

Parameters	Central value (base case)	Upper limit	Lower limit
Pressure (hPA)	330	350	300
Altitude (m)	8500	9000	8000
Temperature (°C)	−51	−50	−52
Relative humidity	85%	93%	84%
Updraft velocity (cm s^{-1})	25	35	15
Vertical displacement (m)	30	35	25
Aerosol number concentration, mode 1	350	500	150
Median diameter of mode 1 (μm)	0.1	0.2	0.05
Geometric standard deviation of mode 1	1.65	1.8	1.5
Aerosol number concentration, mode 2	1	10	0.1
Median diameter of mode 2 (μm)	0.725	0.725	0.725
Geometric standard deviation of mode 2	1.4	1.4	1.4

The aircraft flew at three levels inside the cirrus clouds on 18 March 1994. We focus on the observations made in the middle level (altitude 8500 m, pressure 330 hPa). The average temperature in this level is −15°C. We chose 85% as the initial relative humidity (over water) for air parcel to start with. Eighty-five percent relative humidity is above the deliquesce point of ammonium sulfate particles and close to but smaller than the relative humidity observed inside the cirrus clouds at that level (Fig. 2 of Ström et al. 1997).

Since we are primarily interested in the formation processes of cirrus clouds, we shall examine a single adiabatic uplift. A constant updraft velocity was assumed for the air parcel. We took 25 cm s^{-1}, a velocity close to the average value of the updrafts exceeding zero from the frequency distribution (Ström et al. 1997) of the observed vertical wind in all four flights, as the updraft velocity for the air parcel. The clouds observed on 18 March exhibited a wave structure with amplitude of about 30 m (Ström et al. 1997). We took 30 m as the base-case vertical displacement.

The input aerosol size distributions and number concentration are a composite of both the measured interstitial and residual aerosol size distributions. A lognormal fit of the observation data, shown in Fig. 1, was used as the initial aerosol size distribution for the base-case simulation. The relative parameters for the distribution are given in Table 1. Since the interstitial inlet sampled particles smaller than about 1 μm and the CVI sampled cloud particles larger than 5 μm diameter, this composite distribution is incomplete. The ''gap'' between the CVI and interstitial inlets may cause the number concentration of aerosol particles to be underestimated. Results presented below will show that the shape of the measured aerosol size distribution is unlikely to have been influenced by this gap. The potential error introduced by this gap is likely to be within the bounds of the sensitivity analysis we present, so that our conclusions will not be influenced by the noncomplementary inlets.

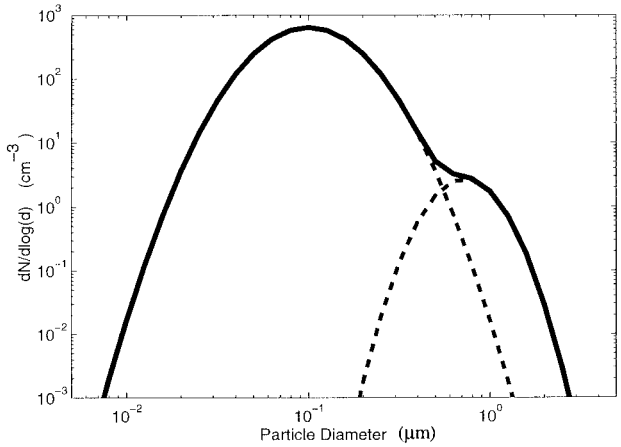

FIG. 1. The lognormal aerosol size distribution with a number concentration of 350 cm^{-3} for the base-case simulation.

b. *Measurement data for comparison of model output parameters*

Ice crystal size distributions were measured using an ice replicator (Hallet 1976). Cirrus cloud particles are impacted onto a moving Formvar-coated film. The Formvar then hardens, preserving the near-original size and shape of the cloud particles. The crystals are identified, counted, and sized on the film using an optical microscope and processing software. The crystal size distributions deduced from replicator data obtained on 18 March 1994 appear to be grouped into two regimes (Ström et al. 1997). The size distributions for these two groups are presented as envelopes of one standard deviation above and below the mean in Fig. 2. The effective radii calculated from the average of these two groups of size distributions are given in Table 2.

Ice water content, residual aerosol size distribution, and ice crystal number concentration were measured using the CVI inlet. Once the cloud particles are sampled by the CVI, they are evaporated in clean, dry, and warm air, leaving behind the cloud water as water vapor and the nonvolatile material that was present in the crystals as residual aerosol particles. There are instruments lo-

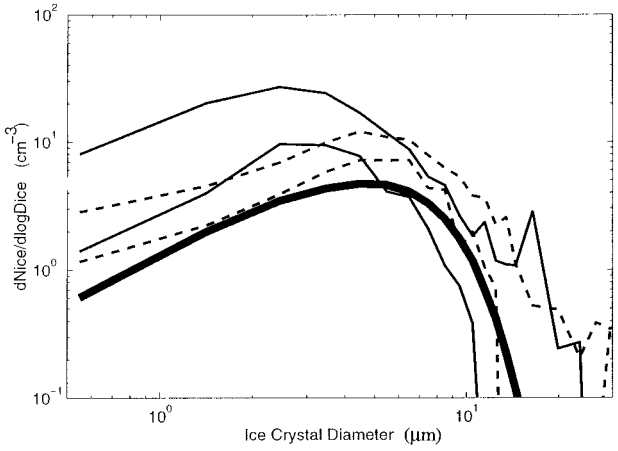

FIG. 2. Calculated ice crystal size distributions (heavy solid line) at 30 m above the starting altitude is shown, along with two envelopes (areas between two solid lines and two dashed lines) of observed crystal size distribution from two regimes observed by using the replicator on 18 March 1994.

cated downstream of the CVI inlet, where ice water content is measured by a dual-beam Lyman-α hygrometer; residual aerosol size distributions and number concentrations are measured using a particle measuring system (PMS) PCASP (Passive Cavity Aerosol Spectrometer) and a CPC (condensation particle counters). Ice crystal number concentrations are inferred from the residual aerosol number concentrations. Typical values of measurements taken in March 1994 by using the CVI are also given in Table 2.

4. Base-case study: Comparison with data measured on 18 March 1994

The central values from the measurements listed in Table 1 were chosen as model input values. A bimodal aerosol size distribution as shown in Fig. 1 was used as the initial dry particle size distribution in the air parcel. These particles were allowed to grow to their equilibrium size in the initial step of the model calculations. The air parcel was then lifted adiabatically, and the particles continued to acquire water as the temperature of the air parcel decreased. Ice crystals formed by homogeneous freezing of the solution droplets. Once ice nucleation has ceased, the crystals continue to grow through vapor diffusion.

a. Ice crystal size distributions and number concentrations

The simulated ice crystal size distribution after a 30-m uplift for the base-case study is shown in Fig. 2 by the heavy solid line. Two envelopes, areas between two dashed lines and two thin solid lines, show the crystal size distributions from two regimes observed on 18 March 1994. The observed crystal sizes were converted to the diameter of an equal volume sphere for comparison with model results. For crystal larger than 5 μm, the model results and experimental data show very good agreement. Both model results and observations indicate the presence of a large number of crystals smaller than 10 μm. The mode in the model crystal size distribution is at 5-μm diameter, close to the measurement values. Since the replicator has a sampling efficiency less than unity for crystals smaller than its lower cut size (approximately 4 μm), it is likely that the model underpredicts the number of crystals of this size actually present in the cloud. The model does not produce large ice crystals (larger than 20 μm) in our base-case simulation. Crystals of this size were rare in the observations of Ström et al. (1997), which indicates that the clouds were in the formation stage.

The model-predicted crystal effective radius R_e, defined as $R_e = \Sigma\, n(r)r^3/\Sigma\, n(r)r^2$, is calculated and shown in Table 2, together with two effective radii derived by using the average of two groups of observed crystal size distributions given in Fig. 2. As we can see, the model-produced crystal effective radius of 3.8 μm is very close to 4 μm, which is the effective radius derived from one of the groups (dashed line in Fig. 2) of observational data.

Another comparison between the model results and observations is the crystal number concentration. The

TABLE 2. Comparison of model output results and observations.

	Model results (base case)	Measurements median values and (ranges)
Ice crystal (>5 μm) number concentration (cm^{-3}, STP*)	2.4	2.5 (0.01–15)
Ice water content (mg m^{-3}, STP)	0.55	6 (0.1–100)
Aerosol scavenging fraction (crystals > 5 μm) (%)	0.27%	0.3% (0.001%–10%)
Ice crystal effective radius (μm)	3.8	4 and 6**

* STP (standard temperature and pressure, 273.15 K and 1013.25 hPa) values in our base-case simulation are about a factor of 2.5 larger than their ambient values.

** These two effective radii were calculated by using the average of two groups of crystal size distributions observed from replicator measurements. Here, 4 μm is the effective radius of crystal distributions presented by dashed lines in Fig. 2, 6 μm for solid lines.

CVI sampled ice crystals larger than 5-μm diameter. Observations from all four flights (total of about 3000 data points) give a range of crystal number concentrations from 0.01 to 15 cm^{-3} STP (standard temperature and pressure, 273.15 K and 1013.25 hPa) and a median crystal concentration of about 2.5 cm^{-3} STP (Table 2). In the base-case simulation, the model predicted a total number concentration of 9 cm^{-3} STP for all ice crystals. For crystals larger than 5-μm diameter (the cut size of the CVI), the model-produced crystal number concentration is 2.4 cm^{-3} STP, very close to the observed median crystal concentration. We have discussed replicator measurement in Fig. 2. The crystal number concentrations for two regimes for crystals larger than 5 μm are 4.1 cm^{-3} STP (solid lines) and 5.8 cm^{-3} STP (dashed lines). These two values are higher than the model-produced crystal number concentration 2.4 cm^{-3} STP and central value of CVI measurement 2.5 cm^{-3} STP. However, they are in the range 0.01–15 cm^{-3} STP of crystal number concentration observed by the CVI.

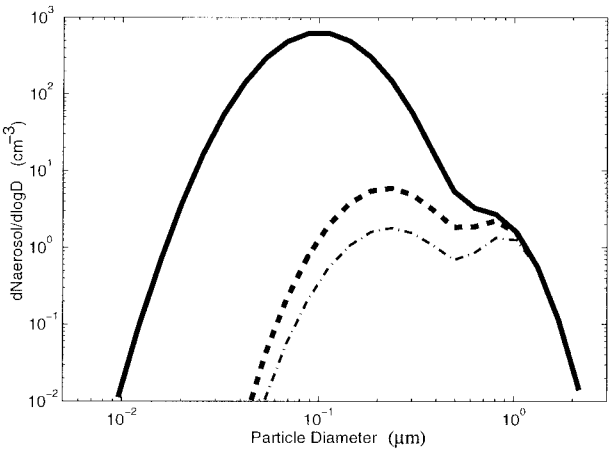

FIG. 3. Model-produced ice crystal residual size distribution (dashed line), input aerosol size distribution (solid line), and calculated residual size distribution for ice crystals 9 μm $< D <$ 10 μm (dashed dotted line).

b. Ice water content

Although the model shows good agreement with ice crystal size distributions and number concentrations, the predicted ice water content (0.55 mg m^{-3} STP) is lower than the measurement median value (6 mg m^{-3} STP). However, it is still within the measurement range (0.1–100 mg m^{-3} STP). We calculated the maximum amount of liquid water that could condense from an air parcel rising 30 m at base-case initial condition to be about 6 mg m^{-3} STP. It is possible that one single uplift did not provide enough time for this water vapor to condense to the ice phase. Another possible reason for discrepancy in ice water content is that the model-produced crystal spectrum did not contain large crystals in the base-case simulation. The discrepancy between the model-predicted and observed ice water contents may also be due to the inhomogeneity of cirrus clouds.

c. Residual aerosol particle size distribution

The CVI used in the field campaign sampled cloud particles larger than 5-μm diameter, excluding interstitial aerosol particles and ambient gases. The sampling efficiency of the CVI has been experimentally determined by Noone et al. (1988) and Anderson et al. (1993). Theoretical and sensitivity studies of the sampling characteristics of the CVI have also been presented in Lin and Heintzenberg (1995) and Lin and Noone (1996). Once the cloud particles were sampled by the CVI, they were evaporated, leaving behind the nonvolatile material that had been present in the crystals as *residual* aerosol particles. Strictly speaking, these particles represent the nonvolatile material upon which the cloud particles formed, plus whatever material the crystals/droplets acquired by coagulation or chemical reaction between the time they formed and when they were sampled. Since the clouds sampled in the Ström et al. (1997) measurements were in the formation stage, the residual aerosol particles most likely reflect the original nuclei for the ice crystals.

The calculated residual aerosol particle size distribution is shown in Fig. 3, together with the model input aerosol size distribution. The residual size distribution has two modes, as does the initial aerosol size distribution. The most striking feature of the results is that particles smaller than 1-μm diameter determine the ice crystal number population. Not only are the larger aerosol particles scavenged by ice crystals, but the smaller ones are as well. For the base case, aerosol particles as small as 0.05 μm are activated. The residual size distribution for crystals in a single size interval (between 9 and 10 μm in diameter) is also plotted in Fig. 3. It is clear that the larger ice crystals are not necessary formed only on larger aerosol particles, as is often the case for droplets in nonprecipitating warm clouds (Noone et al. 1990). Additionally, the shape of the residual particle size distribution for crystals of a single size interval resembles the shape of the residual distribution for the entire range of ice crystal sizes. In the model, this is a result of the stochastic nature of the ice nucleation parameterization. While we have no measurements of the residual particles from a single ice crystal size, the good correspondence between the measured and modeled residual particle distributions for crystals larger than 5 μm suggests that the ice nucleation parameterization is an acceptable description of the actual processes at work in the ambient cloud.

The model-produced residual size distribution can also be compared with CVI measurements as shown in Fig. 4. The area between the two dashed lines represents measured CVI residual size distributions. The heavy dashed line is the calculated residual size distribution for ice crystals larger than 5 μm—the CVI cut size. The

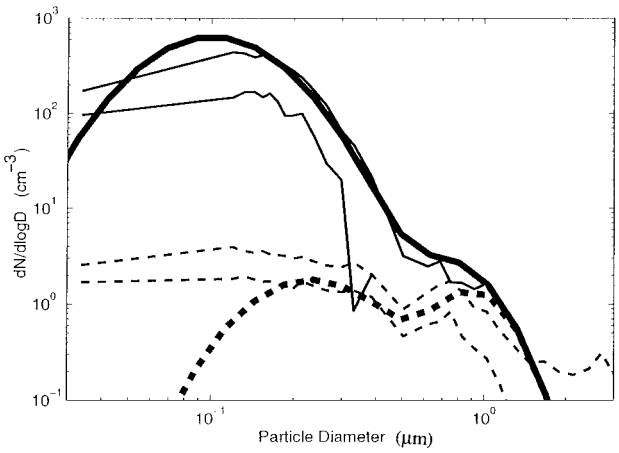

FIG. 4. Comparison of model-produced residual size distribution for crystals larger than the CVI cut size (heavy dashed line) and model initial aerosol input (heavy solid line), together with measured residual size distributions (areas between two dashed lines) and interstitial aerosol size distributions (areas between two solid lines).

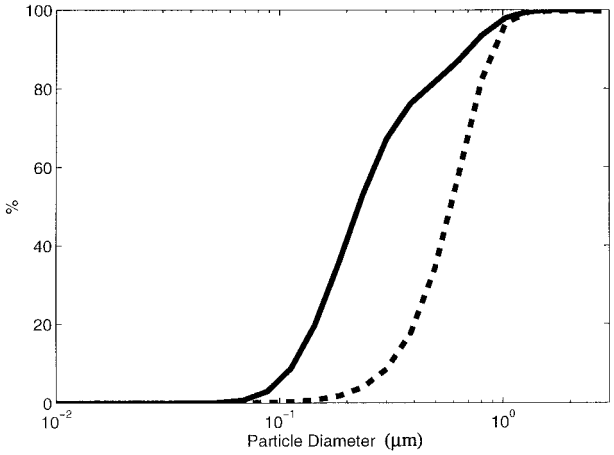

FIG. 5. Aerosol scavenging fraction (dashed line) and cumulative residual size distribution (solid line) as a function of particle size.

model produced a bimodal residual size distribution. Two modes were also observed in the in situ residual particle measurements. The calculated residual size distribution and number concentrations are in very good agreement with the measurement data for aerosol particles larger than 0.2 μm. The model underpredicts the concentration of residuals smaller than 0.2 μm. The modeled concentration decreases rapidly below 0.2 μm, while the measured data did not. It should be noted that there is only one data point in the measurements below 0.1 μm. Similar results in terms of residual particle size distributions have also been presented in Noone et al. (1993) and Ström et al. (1994a) for observations over northern Germany during the International Cirrus Experiment in 1989. The measured interstitial aerosol size distribution is also presented in Fig. 4 by the area between two thin solid lines. The model initial aerosol size distribution, presented by heavy solid line, is the sum of both interstitial and residual size distributions.

There are several interesting aspects of these results. The large ice crystals in cirrus clouds must have started their lives as small crystals. Since submicrometer aerosol particles are seen to have formed small ice crystals in both measurements and model results, it seems that they also play a role in the life cycle of larger ice crystals. As anthropogenic activities are a major source for submicrometer aerosol particles in the industrial regions (Charlson et al. 1992), they must have some influence on the microphysical properties of cirrus clouds.

d. Scavenging fraction of aerosol particles

The fraction of the total number of initial aerosol particles at one size scavenged by cirrus clouds is defined as

$$\text{scavenging fraction } (d) = \frac{\text{number concentration of residuals of diameter } d}{\text{number concentration of initial aerosol of diameter } d}$$

and is shown as a function of particle diameter by dashed line in Fig. 5. The scavenging fraction increases with increasing particle size. For our base case, 50% of aerosol particles with diameter as 0.6 μm are scavenged by cirrus clouds. For aerosol particles larger than 1 μm, more than 90% are scavenged. The cumulative residual size distribution is defined as

$$\text{CRSD}(d) = \frac{\sum \text{number concentration of residuals smaller than } d}{\text{total number concentration of residuals}}$$

and is also plotted as a function of aerosol size in Fig. 5, shown as a solid line. Among these scavenged aerosol particles, 70% were particles smaller than 0.3-μm diameter. Thus, small particles can play an important role in the formation of ice crystals in cirrus clouds. Combining Figs. 1 and 5, the aerosol particles in the first mode (mode diameter 0.1 μm), which dominate the main aerosol number population, are the main source of residual particles. For particles in the second mode (mode diameter 0.7 μm), the chances of being scavenged are higher than for particles in the first mode. Even though the number concentration of particles in the larger mode are quite low (total contribution 1 cm^{-3}), these particles may have a significant contribution to ice crystal number under certain conditions.

By taking the ratio of the total number concentration of residuals to the total number concentration of initial aerosol particles, the total scavenging fraction can be calculated. Totally, only about 1% of initial aerosol particles were scavenged in the formation process. For cirrus crystals larger than 5 μm, the total scavenging fraction of aerosol is 0.27%, which is in the range of CVI

measurement (0.001%–10%) and very close to the median value of 0.3%.

e. Summary of the base-case simulation

In the base-case study, the model-predicted ice crystal size distribution, number concentration, residual size distribution, and aerosol scavenging fraction have shown very good agreement with observations. The model-produced ice water content is also in the measurement range but lower than the median value. A summary of model results is given in Table 2 together with experimental data. The base-case study indicates that cirrus clouds, especially at the early formation stage, can contain large numbers of ice crystals in the range between 0.5 and 20 μm. The aerosol scavenging fraction shows small aerosol particles are activated in ice crystal formation.

5. Model sensitivity study

In this section, the sensitivity of simulated cirrus properties to environmental conditions and aerosol properties will be discussed. Six input parameters, such as air parcel updraft velocity, vertical displacement, aerosol number concentration, size distribution, model initial temperature, and relative humidity, were perturbed individually relative to the base-case values in order to investigate the uncertainties in the base-case simulation that result from the uncertainty involved in not being able to observationally follow a cirrus parcel in a Lagrangian manner. In each simulation, the indicated parameter was changed, and all other input parameters remained same as in the base case. The changes in ice crystal size distributions, crystal number concentrations, and ice water content for each case will then be discussed.

a. Air parcel vertical displacement and updraft velocity

Since we focus on a single adiabatic uplift in a wave-structured cirrus cloud, the vertical displacement of the parcel in the model is related to the amplitude of the waves. The choice of vertical displacement controls the residence time of ice particles in the simulation. A larger vertical displacement gives a longer residence time allowing more crystals to form and grow. The test results for vertical displacements of 25 and 35 m are given in Fig. 6 and Table 3. When the air parcel is lifted 25 m from its initial position, there are 1.4 cm^{-3} ice crystals formed in the air parcel. Crystal number concentration increases to 3.7 cm^{-3} at 30 m (base case) and 5.2 cm^{-3} at 35 m. Actually, the crystal number concentration will keep increasing until it reaches the potential maximum at 40 m, which is beyond the air parcel's vertical displacement discussed in this section. At the develop stage, ice water contents and ice crystal effective radii are all increased with the increasing in air parcel vertical displacement. A relative humidity distribution versus air parcel's vertical displacement is given in Fig. 7. The peak value of relative humidity is reached at 30 m. As the existing ice crystals grow, they deplete water vapor and lower the relative humidity. When relative humidity decreases, the nucleation rate for new ice crystals is slowed down, hence the number concentration for small crystals decreases, which is why the size distribution for the 35-m case (dashed-dotted line in Fig. 6a) shows a lower concentration of small crystals compared with the base case.

By examining the aerosol size at which the scavenging fraction reaches 50%, we find that at 25 m, half of the aerosol particles larger than 0.9-μm diameter are activated (Table 3). At 35 m, the size at which 50% of the aerosol particles are scavenged is as small as 0.5 μm. More aerosol particles are activated as the vertical displacement of the air parcel is increased.

Updraft velocity is an important parameter in the cloud formation process as it is directly related to the large-scale atmospheric dynamic forcing. Two different air parcel updraft velocities were tested when the vertical displacement of the air parcel was fixed in the 30-m case. Ice crystal size distributions for these tests are shown in Fig. 6b. The heavy solid line indicates the ice crystal size distribution for the base case, the dashed-dotted line is for 35 cm s^{-1} updraft velocity, and the dashed line for a 15 cm s^{-1} updraft. As the crystal growth is a time-dependent process, in a fixed vertical displacement case, slower ascents give more time for crystals to grow. This is why with a slower updraft velocity, the crystal size distribution shifts to larger sizes. Crystal number concentrations, ice water contents, and ice crystal effective radii for air parcel starting at different updrafts are also given in Table 3. Crystal number concentration increased from 1.9 to 3.7 cm^{-3} as updraft increased from 15 to 35 cm s^{-1}. Strong updraft tends to nucleate more crystals. However, the ice water content is lower and crystals sizes are smaller at strong updraft in a fix vertical displacement.

b. Aerosol effects on the cirrus formation

The impact of aerosol properties on cirrus formation needs to be understood since aerosol properties in the upper troposphere and lower stratosphere can be influenced by anthropogenic activities. Our base-case simulation and observational studies show that aerosol concentrations are much higher than observed ice crystal number concentrations. The difference may be as much as a factor of 50 or more. In this section, the impact of initial aerosol number concentration and aerosol size distribution to the crystal size distribution will be discussed.

Figure 6c shows the ice crystal size distributions for two tests using different initial aerosol number concentrations. For each test, the initial aerosol size distribution

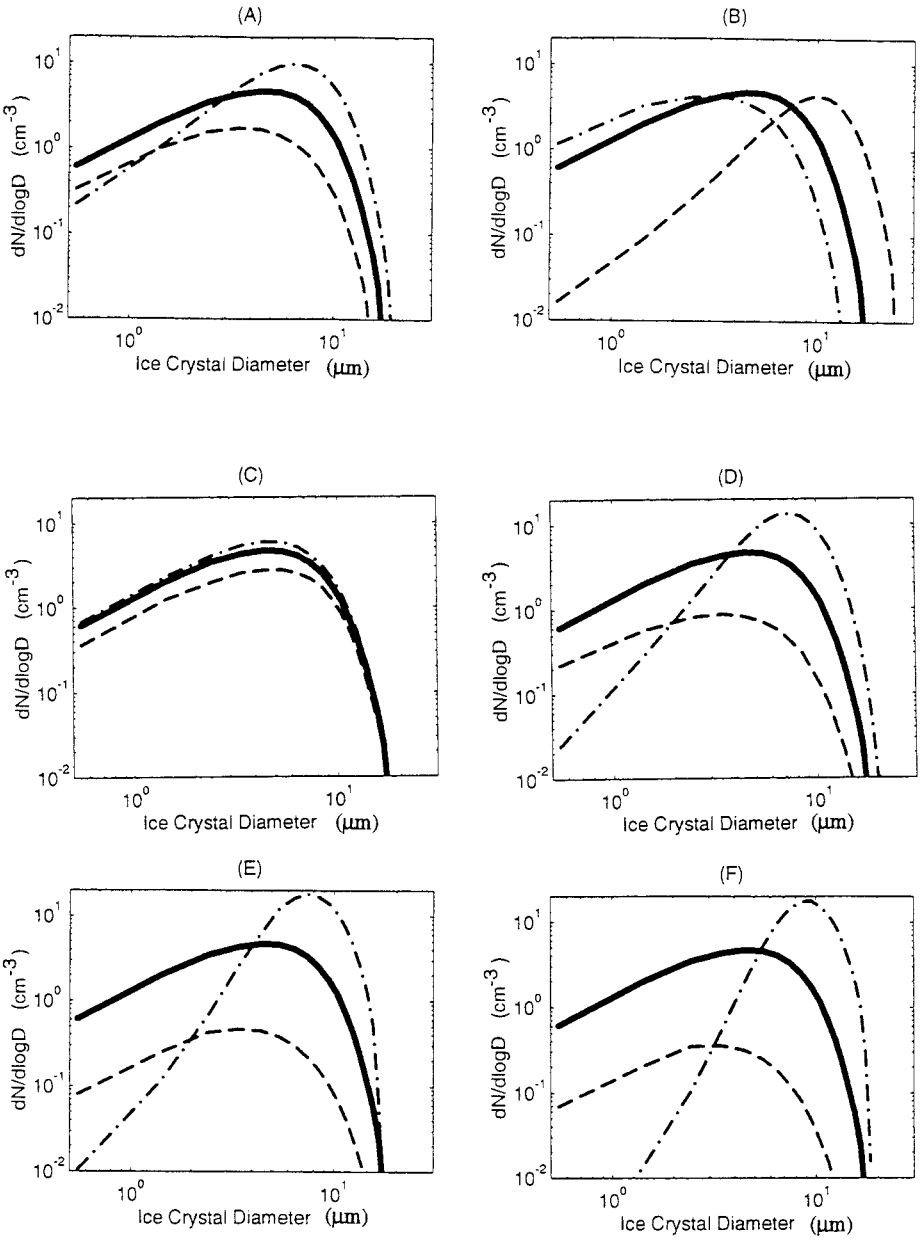

FIG. 6. Crystal size distributions for the model sensitivity study. Six parameters were tested. In each simulation, the indicated parameter was changed, and all other input parameters were same as were used in the base-case study. The solid lines in all figures are the crystal size distributions for the base-case simulation. (a) Ice crystal size distributions at 25 (dashed line), 30 (solid line, base case), and 35 m (dashed-dotted line); (b) crystal size distributions for different initial updraft velocities 15 (dashed line), 25 (solid line, base case) and 35 cm s^{-1} (dashed-dotted line); (c) crystal size distributions for different initial aerosol number concentrations: 150 (dashed line), 250 (solid line, base case), and 500 cm^{-3} (dashed-dotted line); (d) crystal size distributions for different initial aerosol mode diameters: 0.05 (dashed line), 0.1 (solid line, base case), and 0.2 μm (dashed-dotted line); (e) crystal size distributions for different starting temperatures: $-50°$ (dashed line), $-51°$ (solid line, base case), and $-52°$C (dashed-dotted line); (f) crystal size distributions for different initial relative humidities: 84% (dashed line), 85% (solid line, base case), and 86% (dashed-dotted line).

TABLE 3. Results of model sensitivity study. For each case, only one of the initial parameters is perturbed relative to the base case initial value.

	Base case	Vertical displacement (m)		Updraft velocity (cm s^{-1})		Aerosol number concentration (cm^{-3})		Aerosol mode diameter (μm)		Temperature (°C)		Relative humidity (%)		
Initial parameter perturbed relative to the base case		25	35	15	35	150	500	0.05	0.2	−50	−52	84	86	93
Crystal number concentration (cm^{-3})	3.7	1.4	5.2	1.9	3.7	2.2	4.4	0.76	5.6	0.38	6.8	0.28	5.6	348
Ice water content (mg m^{-3})	0.22	0.06	0.68	0.84	0.08	0.14	0.27	0.03	1.0	0.02	1.32	0.01	1.9	17.9
Crystal effective radius (μm)	3.6	3.2	4.2	6.0	2.6	3.7	3.5	3.2	4.5	3.2	4.5	2.9	5.2	2.7

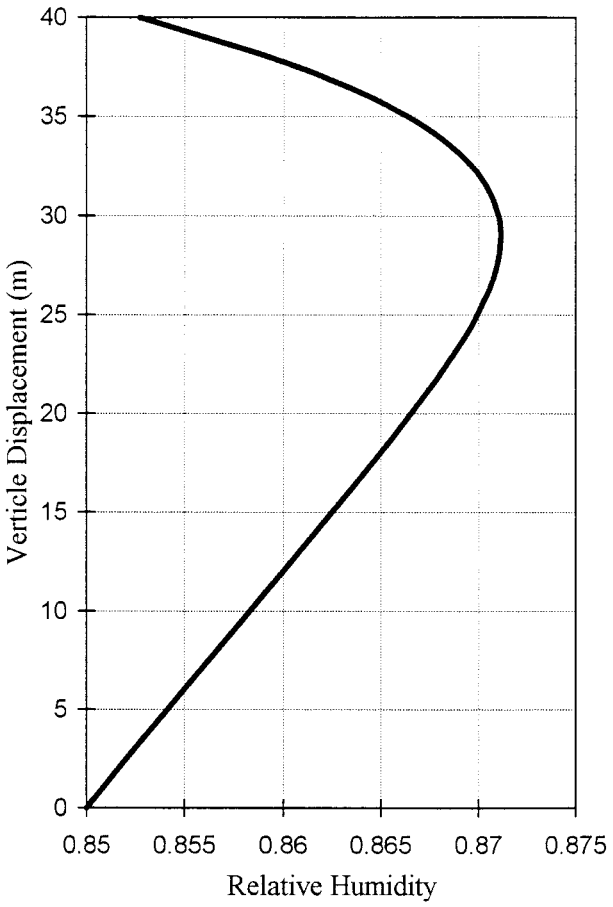

FIG. 7. Vertical distribution of relative humidity for the air parcel starting with a initial condition as base case.

had the same shape as in Fig. 1, but the total concentrations are taken from the upper and lower limits listed in Table 1. The solid line in Fig. 6c indicates the base-case crystal size distribution. The dashed line and dashed-dotted line are the ice crystal size distributions for input aerosol number concentrations of 150 and 500 cm^{-3}, respectively. As initial aerosol concentrations increase from 150 to 500 cm^{-3}, the model-produced crystal size distributions kept similar shapes and their crystal effective radii (given in Table 3) are quite close, but the crystal number concentration almost doubled. The results in Table 3 also shows that the ice water content increased slightly with the increasing total aerosol number concentration.

In this sensitivity study, we also chose to maintain the bimodal shape and number concentration of the initial aerosol size distribution but vary the mode diameters. Mode diameters of mode 1 at 0.05 μm, 0.1 μm (base case), and 0.2 μm were tested. The simulation results presented in Fig. 6d and Table 3 shows that the impact of aerosol sizes on the crystal spectrum is quite significant. For example, there are 5.6 cm^{-3} crystals nucleated for aerosols with mode diameter at 0.2 μm,

but only 3.7 cm^{-3} crystals nucleated for aerosols with mode diameter at 0.1 μm. Larger aerosol particles were more readily scavenged than small aerosol particles in the cirrus formation process.

Again, the aerosol number concentration and their size distribution have impact on the cirrus cloud properties. However, one should keep in mind that these sensitivity tests were carried out by air parcels in a single uplift with an limited vertical displacement. The conclusion may only apply to the wave-structured cirrus clouds where air parcel's vertical displacement is limited.

c. Thermodynamic parameters

The sensitivity of the model results to the input thermodynamic parameters was tested by focusing on air parcel initial temperature, relative humidity, and pressure. Two different initial temperatures, -50°C and -52°C, were chosen as model input and all other input parameters were same as the base case. The crystal size distributions for these two cases are shown together with base-case results in Fig. 6e. When air parcel started at lower temperature, the crystals turned to have a narrower distribution with higher peak on larger crystal side. The values for crystal number concentrations, ice water contents, and crystal effective radii are given in Table 3. Within the air parcel's 30-m uplifting, there are more ice crystals produced when the air parcel started in lower temperature environment and the average crystal size tends to be larger. By changing the temperature 1°, for example from $-51°$ to -52°C, the ice number concentration increases as much as a factor of 2 and the ice water content increases as a factor of 6, which indicates that temperature is one of the sensitive input parameters.

Similar simulations for different initial relative humidities were also tested with all other input parameters and air parcel vertical displacement the same as the base case. Figure 6f shows the ice crystal size distribution for initial relative humidities taken as 84%, 85% (base case), and 86%. Ice crystal sizes and number concentrations increase with increasing initial relative humidity. Table 3 also shows that an increase in initial relative humidity also increases crystal number concentrations, ice water contents, and crystal effective radii. Relative humidity is a sensitive input parameter.

The base-case relative humidity profile has been given in Fig. 7. Starting with an initial value of 85%, relative humidity reached its peak value of 87.1% at 30 m. The average relative humidity observed in the middle level in cirrus clouds on 18 March 1994 is 95% with $\pm$10% instrument uncertainty (Ström et al. 1997). It is obvious that the relative humidity in the base-case simulation is lower than the average values from observation. The peak values of two other tests starting with 84% and 86% only reached 87% and 87.2%, respectively. The relative humidity achieved by the air parcel is still below the average of observed values. Two explanations could be made for the relative humidity discrepancy between model simulation and observation. The discrepancy may have been caused by the uncertainty in crystal nucleation rate. However, for this case, the discrepancy is more likely caused by the uncertainty of instrument used for relative humidity observations. In the campaign, relative humidity was measured by using a cryogenically cooled frost point mirror (Busen and Buck 1993; Ström et al. 1994b). The $\pm$10% instrument uncertainty has been discussed by Ström et al. (1994b) and Ström et al. (1997), and it was concluded that it is possible the humidity data is systematically overestimated by as much as 10%. Further, an air parcel starting with a relative humidity of 93% has also been tested and results are given in Table 3. The crystal number concentration increased significantly to 348 cm^{-3}. Almost all of the initial aerosol particles (350 cm^{-3}) are scavenged to form ice crystals. The crystal number concentration is too high to be realistic for cirrus clouds. Some ice crystals must have formed and deplete the water vapor in the air parcel before it reaches a relative humidity of 93%. To summarize, the model simulation not only showed that the relative humidity is a sensitive input parameter for the model simulation, but also supported the explanation that there is a 10% bias in observed relative humidity.

Different initial values of model input pressure were also tested. The results show that pressure is not a sensitive parameter in the model simulation.

d. Summary of sensitivity tests

Sensitivity tests for the different model input parameters based on limits listed in Table 1 have been performed. For an air parcel with a single uplift of 30 m, temperature and relative humidity are the most sensitive input parameters. A 1° decrease in initial temperature could cause crystal number concentration increase or decrease by a factor of 2 or even 10. Air parcel updraft velocity is also a sensitive parameter. The higher the updraft velocity, the more ice crystals are nucleated, but the nucleated crystals may not have enough time to grow to large ice crystals if the vertical displacement is limited. The aerosol size distribution and total aerosol number concentration also affect the ice crystal size distribution but not as dramatically as temperature.

6. Summary and conclusions

In this study, we simulated cirrus clouds observed during March 1994 over southern Germany. A modified air parcel model with homogeneous nucleation of ice crystals was used for the simulation and sensitivity tests. As the clouds observed on 18 March exhibited a wave structure with amplitude of about 30 m (Ström et al. 1997), the cirrus formation processes in the air parcel was examined by a single adiabatic uplift with limited

vertical displacement. Typical data measured on 18 March 1994 were chosen for a base-case simulation and for model results comparison. Sensitivity tests were performed using the range of measured values during the same campaign. The major conclusions of this study are given below. However, one should keep in mind that some conclusions may only apply to the cirrus formation in the wave-structured clouds where the air parcel's vertical displacement is limited.

- Large numbers of small ice crystals (between 0.5 and 20 μm) were found in the model results. The predicted ice crystal size distributions and number concentrations agreed very well with observed values.
- Aerosol particles as small as 0.05 μm were found to have been activated in the cirrus formation process. For our base-case simulation, 1% of the total number of aerosol particles were scavenged by the cirrus clouds. Of these scavenged particles, 70% were smaller than 0.3 μm.
- The residual particle size distribution was bimodal, as was the residual distribution for ice crystals in a single size interval. The simulated residual size distributions and number concentrations agreed well with observations from 18 March 1994.
- There was no strong link between the sizes of ice crystals and the sizes of residual particles. The larger ice crystals did not necessarily form on the larger aerosol particles.
- Ice crystal number concentration increases with increasing initial aerosol number concentration. Only between 1% and 2% of the total number of aerosol particles were scavenged by the cirrus clouds.
- The most sensitive model environmental parameters affecting ice crystal size distributions are temperature, relative humidity, updraft velocity, and aerosol size distribution.
- Higher updraft velocities tend to activate more small aerosol particles, producing a higher crystal concentration. Lower updraft velocities produce larger ice crystals.
- Ice crystal number concentrations and crystal effective radius values increase with increasing initial relative humidity or decreasing initial temperature.
- The predicted cirrus ice water content is in the measurement range but somewhat lower than the median value observed.

Starting with values of environmental parameters in the range of observations and appropriate aerosol characteristic, the model produced many of the observed young cirrus characteristics including ice crystal size distribution, number concentration, residual size distribution, residual number concentration, and also the total aerosol scavenging fraction. However, model-produced ice water content is somewhat lower than the observed median value, which may relate with the presence of large ice crystals. We suggest the following for future studies.

- Homogeneous nucleation theory may not be a complete description of ice crystal formation and growth. Heterogeneous freezing should also be investigated.
- In our base-case simulation, we focused on a single uplift. As the wave motions were observed in the in situ measurements, the changing updraft velocity might be related to the production of larger ice crystals. Examinations of the dynamic influences on cirrus formation should be carried out in future work.

Acknowledgments. We would like to thank Dr. Larry Miloshevich for many useful discussions of the air parcel model. We are indebted to Prof. Jost Heintzenberg, Klaus Wyser, Dr. Theodore Anderson, and Dr. Robert Nissen for their comments on the manuscript. Support from Prof. Hans-Christen Hansson and Dr. W. Richard Leaitch is appreciated.

REFERENCES

Anderson, T. L., R. J. Charlson, and D. S. Covert, 1993: Calibration of a counterflow virtual impactor at aerodynamic diameters from 1 to 15 μm. *Aerosol Sci. Technol.,* **19,** 317–329.

Busen, R., and A. L. Buck, 1993: A high performance hygrometer for air craft use: Description, installation, and flight data. Institute für Physik der Atmosphäre Rep. 10, 29 pp. [Available from Institute für Physik der Atmosphäre, Oberpffaffenhofen, D-82234 Weßling, Germany.]

Charlson, R. J., S. E. Schwartz, J. M. Hales, R. D. Cess, J. A. Coakley Jr., J. E. Hansen, and D. J. Hofmann, 1992: Climate forcing by anthropogenic aerosols. *Science,* **255,** 423–429.

DeMott, Paul J., M. P. Meyers, and W. R. Cotton, 1994: Parameterization and impact of ice initiation processes relevant to numerical model simulations of cirrus clouds. *J. Atmos. Sci.,* **51,** 77–90.

Dowling, D. R., and L. F. Radke, 1990: A summary of the physical properties of cirrus clouds. *J. Appl. Meteor.,* **29,** 970–978.

Hallett, J., 1976: Measurement of size, concentration and structure of atmospheric particulates by the airborne continuous particle replicator. Report AFGL-TR-76-0149, 92 pp. [Available from Desert Research Institute, University of Nevada System, Reno, NV 89507.]

Heymsfield, A. J., and R. M. Sabin, 1989: Cirrus crystal nucleation by homogeneous freezing of solution droplets. *J. Atmos. Sci.,* **46,** 2252–2264.

——, and L. M. Miloshevich, 1993: Homogeneous ice nucleation and supercooled liquid water in orographic wave clouds. *J. Atmos. Sci.,* **50,** 2335–2353.

——, and ——, 1995: Relative humidity and temperature influences on cirrus formation and evolution: Observations from wave clouds and FIRE II. *J. Atmos. Sci.,* **52,** 4302–4326.

Jensen, E. J., O. B. Toon, D. L. Westphal, S. Kinne, and A. J. Heymsfield, 1994a: Microphysical modeling of cirrus 1: Comparison with 1986 FIRE IFO measurements. *J. Geophys Res.,* **99D,** 10 421–10 442.

——, ——, ——, ——, and ——, 1994b: Microphysical modeling of cirrus 2: Sensitivity studies. *J. Geophys. Res.,* **99D,** 10 443–10 454.

Kinne, S., T. P. Ackerman, A. J. Heymsfield, F. P. J. Valero, K. Sassen, and J. D. Spinhirne, 1992: Cirrus microphysics and radiative transfer: Cloud field study on 28 October 1986. *Mon. Wea. Rev.,* **120,** 661–684.

Lin, H., and J. Heintzenberg, 1995: A theoretical study of the counterflow virtual impactor. *J. Aerosol Sci.,* **26,** 903–918.

——, and K. J. Noone, 1996: A simulation of cloud formation and

sampling using the counterflow virtual impactor. *Contrib. Atmos. Phys.,* **69,** 321–332.

Liou, K. N., 1986: Influence of cirrus clouds on weather and climate processes: A global perspective. *Mon. Wea. Rev.,* **114,** 1167–1199.

Noone, K. B., K. J. Noone, J. Heintzenberg, J. Ström, and J. A. Ogren, 1993: In situ observations of cirrus cloud microphysical properties using the counterflow virtual impactor. *J. Atmos. Oceanic Technol.,* **10,** 294–303.

Noone, K. J., J. A. Ogren, J. Heintzenberg, R. J. Charlson, and D. S. Covert, 1988: Design and calibration of a counterflow virtual impactor for sampling of atmospheric fog and cloud droplets. *Aerosol Sci. Technol.,* **8,** 235–244.

——, ——, and ——, 1990: An examination of clouds at a mountaintop site in central Sweden: The distribution of solute within cloud droplets. *Atmos. Res.* **25,** 3–15.

Ogren, J. A., J. Heintzenberg, and R. J. Charlson, 1985: In situ sampling of clouds with a droplet to aerosol converter. *Geophys. Res. Lett.,* **12,** 121–124.

Sassen, K., and G. C. Dodd, 1989: Haze particles nucleation simulations in cirrus clouds, and applications for numerical modeling and lidar studies. *J. Atmos. Sci.,* **46,** 3005–3014.

Schröder, F., and J. Ström, 1995: Aircraft measurements of sub micrometer aerosol particles (>7 nm) in the midlatitude free troposphere and tropopause region. F.L. thesis, Department of Meteorology, Stockholm University, 22 pp.

Starr, D. O., and S. Cox, 1985: Cirrus clouds. Part I: A cirrus cloud model. *J. Atmos. Sci.,* **42,** 2663–2681.

Ström, J., and J. Heintzenberg, 1994: Water vapor, condensed water, and crystal concentration in orographically influenced cirrus clouds. *J. Atmos. Sci.,* **51,** 2368–2383.

——, ——, K. J. Noone, K. B. Noone, J. A. Ogren, F. Albers, and M. Quante, 1994a: Small crystal in cirriform clouds: A case study of residue size distribution, cloud water content and related cloud properties. *Atmos. Res.,* **32,** 125–141.

——, R. Busen, M. Quante, B. Guillemet, P. R. A. Brown, and J. Heintzenberg, 1994b: Pre-EUCREX intercomparison of airborne humidity measuring instruments. *J. Atmos. Oceanic Technol.,* **11,** 1392–1399.

——, B. Strauss, F. Shröder, T. Anderson, J. Heintzenberg, and P. Wendling, 1997: In situ observations of the microphysical properties of young cirrus clouds, *J. Atmos. Sci.,* **54,** 2542–2553.

Zender, C. S., and J. T. Kiehl, 1994: Radiative sensitivities of tropical anvils to small ice crystals. *J. Geophys. Res.,* **99,** 25 869–25 880.